Chemical Science

EDGE ARTICLE

View Article Online
View Journal | View Issue

Cite this: *Chem. Sci.*, 2019, **10**, 6689

All publication charges for this article have been paid for by the Royal Society of Chemistry

Turn on of sky-blue thermally activated delayed fluorescence and circularly polarized luminescence (CPL) *via* increased torsion by a bulky carbazolophane donor†

Nidhi Sharma,‡[ab] Eduard Spuling,‡[c] Cornelia M. Mattern,[c] Wenbo Li,[b] Olaf Fuhr,[d] Youichi Tsuchiya,[ef] Chihaya Adachi,[efgh] Stefan Bräse,*[ci] Ifor D. W. Samuel*[b] and Eli Zysman-Colman*[a]

The carbazolophane (Czp) donor unit (indolo[2.2]paracyclophane) is introduced to the design pool of donors in thermally activated delayed fluorescence emitters. The increased steric bulk of the annelated donor unit forces an increased torsion between the carbazole and the aryl bridge resulting in a decreased ΔE_{ST} and an enhancement of the thermally activated delayed fluorescence in the triazine-containing emitter **CzpPhTrz**. Further, the closely stacked carbazole and benzene units of the paracyclophane show through-space π–π interactions, effectively increasing the spatial occupation for the HOMO orbital. The chiroptical properties of enantiomers of [2.2]paracyclophane reveal mirror image circular dichroism (CD) and circularly polarized luminescence (CPL) with g_{lum} of 1.3×10^{-3}. ***rac*-CzpPhTrz** is a sky-blue emitter with λ_{PL} of 480 nm, a very small ΔE_{ST} of 0.16 eV and high Φ_{PL} of 70% in 10 wt% doped **DPEPO** films. Sky blue-emitting OLEDs were fabricated with this new TADF emitter showing a high maximum EQE of 17% with CIE coordinates of (0.17, 0.25). A moderate EQE roll-off was also observed with an EQE of 12% at a display relevant luminance of 100 cd m^{-2}. Our results show that the Czp donor contributes to both a decreased ΔE_{ST} and an increased photoluminescence quantum yield, both advantageous in the molecular design of TADF emitters.

Received 12th April 2019
Accepted 28th May 2019

DOI: 10.1039/c9sc01821b

rsc.li/chemical-science

Introduction

Organic Thermally Activated Delayed Fluorescence (TADF) materials have come to the fore as attractive alternative emitters in Organic Light-Emitting Diodes (OLEDs) as they, like current state-of-the-art phosphorescent emitters, can recruit 100% of the generated excitons into light.[1] Since 2012, there are numerous examples in the literature of OLEDs using TADF emitters.

TADF in typical donor–acceptor (D–A) emitters is facilitated by a small singlet-triplet excited state energy difference, ΔE_{ST}, a consequence of the small exchange integral between spatially separated frontier molecular orbitals. The molecular design frequently relies on large torsions between the donor, where the highest occupied molecular orbital (HOMO) resides and the bridging arene and/or between the bridge and the acceptor, where the lowest unoccupied molecular orbital (LUMO) is located. It becomes more difficult to adhere to this design paradigm in blue TADF emitters due to the reliance on weak

[a]*Organic Semiconductor Centre, EaStCHEM School of Chemistry, University of St Andrews, St Andrews, Fife, KY16 9ST, UK. E-mail: eli.zysman-colman@st-andrews.ac.uk*

[b]*Organic Semiconductor Centre, SUPA, School of Physics and Astronomy, University of St Andrews, North Haugh, St Andrews, KY16 9SS, UK. E-mail: idws@st-andrews.ac.uk*

[c]*Institute of Organic Chemistry (IOC), Karlsruhe Institute of Technology (KIT), Fritz-Haber-Weg 6, 76131 Karlsruhe, Germany. E-mail: braese@kit.edu*

[d]*Institute of Nanotechnology (INT) and Karlsruhe Nano-Micro Facility (KNMF), Karlsruhe Institute of Technology, Hermann-von-Helmholtz-Platz 1, D-76344 Eggenstein-Leopoldshafen, Germany*

[e]*Center for Organic Photonics and Electronics Research (OPERA), Kyushu University, 744 Motooka, Nishi-ku, Fukuoka 819-0395, Japan*

[f]*JST, ERATO, Adachi Molecular Exciton Engineering Project, Kyushu University, 744 Motooka, Nishi-ku, Fukuoka 819-0395, Japan*

[g]*Department of Chemistry and Biochemistry, Kyushu University, 744 Motooka, Nishi-ku, Fukuoka 819-0395, Japan*

[h]*International Institute for Carbon Neutral Energy Research (WPI-I2CNER), Kyushu University, 744 Motooka, Nishi-ku, Fukuoka 819-0395, Japan*

[i]*Institute of Toxicology and Genetics (ITG), Karlsruhe Institute of Technology (KIT), Hermann-von-Helmholtz-Platz 1, D-76344 Eggenstein-Leopoldshafen, Germany*

† Electronic supplementary information (ESI) available: CCDC 1871934 and 1871935. For ESI and crystallographic data in CIF or other electronic format see DOI: 10.1039/c9sc01821b. The research data supporting this publication can be accessed at https://doi.org/10.17630/530b50cb-3a77-4256-b5fe-47917e7eaae6

‡ Nidhi Sharma and Eduard Spuling contributed equally to this work.

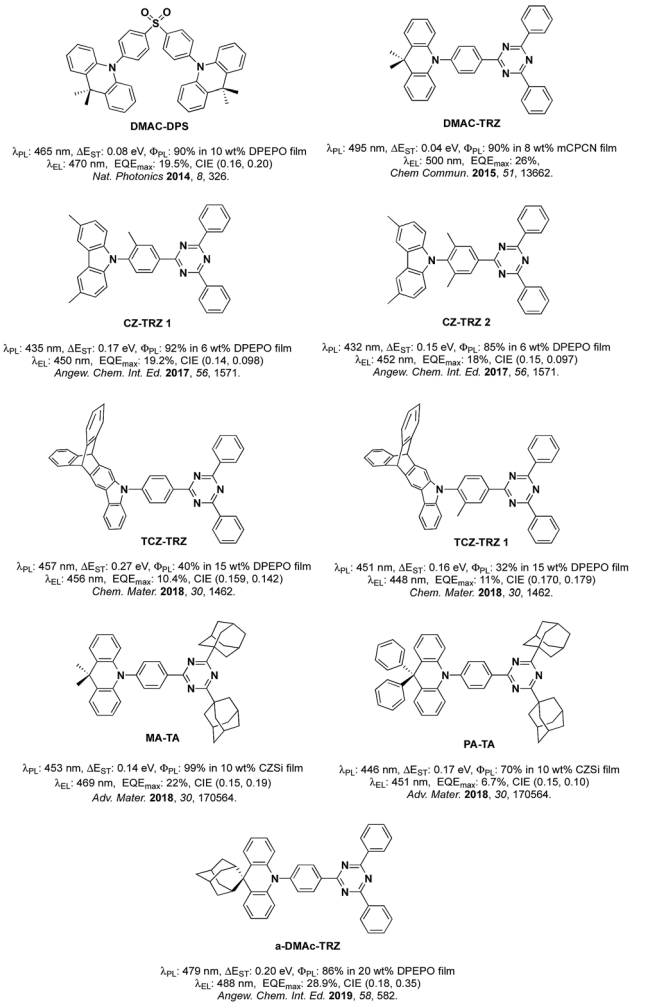

Fig. 1 Chemical structures and performance of known blue and triazine-based TADF emitters.

carbazole (Cz) donors. The inherent size of Cz often results in much shallower torsions thereby leading to increased conjugation within the emitter and a larger ΔE_{ST}. Methylation of either Cz and/or the bridge has been explored as a strategy to combat the propensity for Cz to conjugate to the arene bridge.[2] The state-of-the-art emitters based on the diphenyltriazine (cyaphenine) acceptor moiety in Fig. 1 illustrate these design principles. The methylation of bridging arene induced large torsions of between 71.2° and 82.3° in deep blue emitters **Cz-Trz 1** and **Cz-Trz 2**, reported by Adachi *et al.* OLEDs using these emitters exhibited maximum external quantum efficiencies, EQE_{max} of 19.2 and 18.3% with CIE coordinates of (0.148, 0.09) and (0.15, 0.097) for **Cz-TrZ 1** and **Cz-Trz 2**, respectively. Van Voorhis, Swager, Baldo, Buchwald *et al.*[3] conducted a similar study using a triptycene extended carbazolyl donor unit (**TCZ-TRZ**), which showed a reduced overlap of the frontier orbitals than with the parent Cz donor-based emitter. Larger torsions were obtained through methyl substitution of the bridging arene (**TCZ-TRZ 1**). The photoluminescence quantum yield, Φ_{PL}, in these blue-emitting compounds is significantly decreased compared to those reported by Adachi *et al.*[2a] OLEDs showed EQE_{max} values of 10.4 and 11% and CIE coordinates of (0.159, 0.142) and (0.170, 0.179) for **TCZ-TRZ** and **TCZ-TRZ 1**, respectively.

An alternative approach to functionalizing the weak Cz donor and arene bridge moieties of blue TADF compounds to control the balance of small ΔE_{ST} and high S_1 energy is to employ a stronger, bulkier donor such as dimethylacridine (DMAC).[4] For example, employing DMAC in combination with a diphenylsulfone acceptor (**DMAC-DPS**, Fig. 1) resulted in sky-blue emission with EQE_{max} and CIE coordinates of 19.5% and (0.16, 0.20).[5] Upon changing the acceptor to diphenyltriazine in **DMAC-TRZ**, green emission (λ_{EL} = 500 nm) was obtained with EQE_{max} as high as 26%.[6] Incorporation of adamantyl groups onto the cyaphenine acceptor (**MA-TA**, Fig. 1) resulted in a significant blue-shift in the emission and OLEDs with this emitter showed high EQE_{max} of 22% and CIE coordinates of (0.15, 0.19).[4] When the donor was modified to 9,9-diphenyl-9,10-dihydroacridine (**PA-TA**), emission was further blue-shifted with CIE coordinates of (0.15, 0.10). However, the efficiency of the device suffered and the EQE_{max} was limited to 6.7%. Recently, an adamantyl-substituted acridine donor was introduced by Su *et al.*[7] and coupled with a triazine acceptor. The rigid backbone of the donor in **a-DMAc-TRZ** suppressed nonradiative decay processes. Dual emission was observed from two conformers with an EQE_{max} of 28.9% and CIE of (0.18, 0.35).

Circularly polarized luminescence (CPL) enabled chiral molecules have been widely investigated for their potential applications in optical data storage[8] and optical spintronics.[9] In terms of display applications, such molecules are appealing especially in the development of circularly polarized OLEDs (CPOLEDs). At present, flat panel OLED-based display technologies require a film composed of a polarizer and a quarter wave plate to reduce the reflectance from the surroundings to a minimum in order to achieve high signal-to-noise contrast ratio.[10] Such a solution is however inefficient as the polarizer absorbs half of the emission from an OLED. Such losses can be mitigated if there is CPL. CPL-active small organic molecules (CPL-SOMs), mainly fluorescent compounds, have been investigated in this context; however, currently only a small number of CPL-SOMs are efficient both in terms of high photoluminescence quantum yield (Φ_{PL}) and luminescence dissymmetry factor (g_{lum}).[11] Recently, a number of TADF-based CPL-SOMs have been reported (Fig. S1†). For example, Hirata *et al.* described a TADF CPL emitter, **DPHN**,[12] by introducing a stereogenic carbon center between the donor and acceptor. This g_{lum} for this compound was 1.1×10^{-3}, but there was a very low Φ_{PL} of 4% in toluene. Pieters *et al.*[13] enabled CPL emission in the TADF emitter ***R*-1** through the incorporation of a BINOL unit that confers axial chirality to the molecule. The resulting compound exhibited g_{lum} of 1.3×10^{-3}, a high Φ_{PL} of 53% in toluene and OLEDs displayed EQE_{max} of 9.1%. A chiral *trans*-1,2-diaminocyclohexane was used to link two imide-based TADF emitters in **CAI-Cz.**[14] Each enantiomer showed a g_{lum} value of 1.1×10^{-3} and Φ_{PL} as high as 98%. The resulting CPOLEDs exhibited excellent performances with an EQE_{max} of 19.8% with g_{EL} values of -1.7×10^{-3} and 2.3×10^{-3} for the two enantiomers. Tang *et al.*[15] used a similar design to that of Pieters *et al.* However, in

their design they combine in a single emitter **BN-CF** TADF, AIE (aggregation-induced emission) and CPL properties. **BN-CF** showed a g_{lum} of 1.2×10^{-2}, Φ_{PL} of 32% in toluene, and the CPOLEDs exhibited an EQE_{max} of 9.3% and g_{EL} of 2.6×10^{-2}. Recently, Zhao *et al.*[16] explored the inherent planar chirality of a [2.2]paracyclophane moiety. Emitter **g-BNMe$_2$-C$_p$** exhibited g_{lum} of 4.24×10^{-3} and Φ_{PL} of 46% in toluene.

Results and discussion

We recently demonstrated the first use of a [2.2]paracyclophane bridge within the design of TADF emitters where we exploited the π-stacking interactions of the two arene decks to moderate the electronic coupling of donor and acceptor groups.[17] In this report, we demonstrate an effective design strategy to obtain both TADF and CPL in [2.2]paracyclophanes (**PCP**). We exploit the **PCP** to modulate the torsional angle of the donor with respect to the bridge and its inherent strength and thereby enhance the reverse intersystem crossing (RISC) efficiency in **CzpPhTrz** compared to the reference emitter **CzPhTrz** (Fig. 2). Further, the π–π stacking within the **PCP** enhances HOMO delocalization, thereby increasing the donor strength. Our donor design concept is based on an indole-annelated [2.2] paracyclophane, providing the carbazolophane (**Czp**, [2]paracyclo[2](1,4)carbazolophane). This compact skeleton features a closely coplanar stacked benzene unit on top of a carbazole bridged by two ethylene linkers that slightly bend the arenes from planarity. The short deck distance enables a through-space π–π interaction thereby delocalizing the HOMO and perturbing the electronics and strengthening the donor. We further exploited the inherent planar chirality of the **PCP** scaffold to develop enantiopure TADF chromophores, (R_P)-**CzpPhTrz** and (S_P)-**CzpPhTrz**. We report the chiroptical properties of the enantiomers both in the ground and excited states with circular dichroism (CD) and CPL spectroscopy, respectively. The photophysical investigations of (*rac*)-**CzpPhTrz** revealed its excellent TADF properties with a small ΔE_{ST} of 0.16 eV, a value smaller than those previously reported in Fig. 1, and a high photoluminescence quantum yield, Φ_{PL}, of 69% in 10 wt% **DPEPO** doped films. OLEDs fabricated using (*rac*)-**CzpPhTrz** showed sky blue emission with EQE_{max} as high as 17% and CIE coordinates of (0.17, 0.25). The impact of this donor is clear when compared to the OLED using (*rac*)-**CzPhTrz**, which exhibited a blue-shifted emission with CIE coordinates of (0.14, 0.12) along with a much lower EQE_{max} of 5.8%.

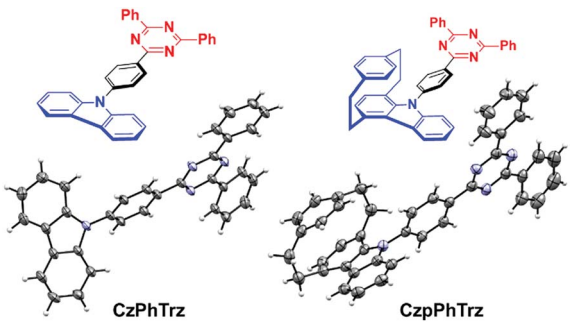

Fig. 2 Carbazol(ophan)yl triazine TADF emitters with molecular structures of **CzPhTrz** (left) and (*rac*)-**CzpPhTrz** (right) drawn at 50% probability level.

Synthesis

The **Czp** donor was synthesized according to the protocol described by Bolm et *al.*[18] (see ESI†). Emitters **CzPhTrz** and (*rac*)-**CzpPhTrz** were obtained in fair and good yields of 42% and 84%, respectively following nucleophilic aromatic substitution of the respective donors with fluorophenyltriazine. Both emitters were purified using a combination of column chromatography, recrystallization and gradient sublimation.§

The structures of both emitters were unequivocally determined by single crystal X-ray diffractometry (Fig. 2). The presence of the cyclophane in (*rac*)-**CzpPhTrz** induces a torsion of 55.86° between the planes of the **Czp** donor and the phenyl bridge while the corresponding torsion in **CzPhTrz** is significantly shallower at 45.11°. The distance between decks in the **PCP** core is 3.07 Å at the N-connected carbon atom, which is consistent with distances in both the free carbazolophane[18] (3.06 Å) and nonsubstituted [2.2]paracyclophanes (3.08–3.10 Å).[19]

Thermal gravimetric analysis (TGA) and differential scanning calorimetry (DSC) were employed to assess the thermal stability of (*rac*)-**CzpPhTrz** (Fig. S8†). (*rac*)-**CzpPhTrz** exhibited excellent thermal stability with a decomposition temperature, T_d, corresponding to a 5% weight loss, of 360 °C, which is a little higher than 330 °C measured for **CzPhTrz**. **CzPhTrz** and (*rac*)-**CzpPhTrz** exhibited melting temperatures, T_m of 270 °C and 263 °C, respectively, ensuring the formation of stable films of both emitters by vacuum deposition. The presence of a **PCP** structural unit introduces planar chirality to the emitter. Enantiomeric emitters (R_P)-**CzpPhTrz** and (S_P)-**CzpPhTrz** were also obtained. These were synthesized from the chiral **Czp** intermediates, which

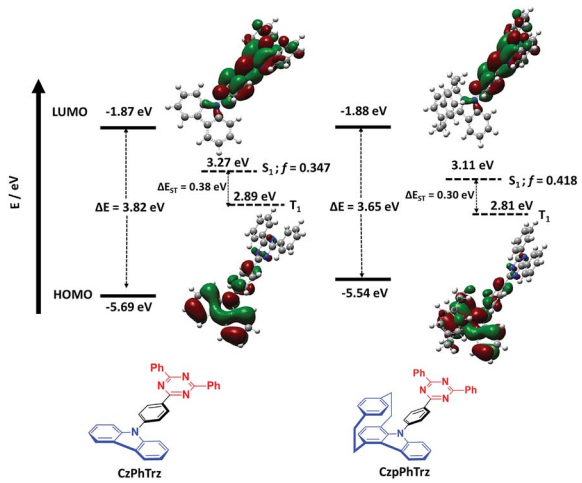

Fig. 3 DFT [PBE0/6-31G(d,p)] calculated ground and TDA-based excited state energies and electron density distributions of the HOMOs and LUMOs of **CzPhTrz** (left) and **CzpPhTrz** (right), *f* is the oscillator strength.

Table 1 Photophysical and electrochemical properties of **CzPhTrz** and **CzpPhTrz**

	λ_{abs}[a], [nm]	λ_{PL}[a], [nm]	Φ_{PL}[b], [%]	λ_{PL}[c], [nm]	Φ_{PL}[c], [%]	τ_p[c], [ns]	τ_d[c], [μs]	HOMO[d,e], [eV]	LUMO[d,e], [eV]	ΔE_{redox}[f], [eV]	S_1/T_1[g], [eV]	ΔE_{ST}[g], [eV]
CzPhTrz	363	446	60 (58)	448	50	4.8	—	−6.11	−3.26	2.86	3.14/2.82	0.32
CzpPhTrz	375	470	70 (55)	482	69	7	65	−5.80	−3.23	2.58	2.89/2.73	0.16

[a] In PhMe at 298 K. [b] Quinine sulfate (0.5 m) in H_2SO_4 (aq) was used as the reference (Φ_{PL}: 54.6%, λ_{exc} = 360 nm).[15] Values quoted are in degassed solutions, which were prepared by three freeze-pump-thaw cycles. Values in parentheses are for aerated solutions, which were prepared by bubbling air for 10 min. [c] Thin films were prepared by vacuum depositing 10 wt% doped samples in **DPEPO** and values were determined using an integrating sphere (λ_{exc} = 360 nm); degassing was done by N_2 purge for 10 minutes. [d] In DCM with 0.1 m $[n\text{Bu}_4\text{N}]\text{PF}_6$ as the supporting electrolyte and Fc/Fc^+ as the internal reference (0.46 V *vs.* SCE).[16] [e] The HOMO and LUMO energies were determined using $E_{HOMO/LUMO} = -(E^{ox}_{pa,1}/E^{red}_{pc,1} + 4.8)$ eV (ref. 17) where E^{ox}_{pa} and E^{red}_{pc} are anodic and cathodic peak potentials, respectively. [f] $\Delta E_{redox} = |E_{HOMO} - E_{LUMO}|$. [g] Determined from the onset of prompt and delayed spectra of 10 wt% doped films in **DPEPO**, measured at 77 K (λ_{exc} = 355 nm).

were separated by chiral HPLC. The absolute configuration could be unambiguously assigned by CD (see ESI† Section 5).

Theoretical properties

Density Functional Theory (DFT) calculations were conducted on both **CzPhTrz** and **CzpPhTrz** (Fig. 3) in order to gain insight into the impact of the use of the **Czp** donor on the optoelectronic properties of the emitters. In both emitters, the HOMO is localized on the carbazole-based donor with some contribution extending onto the phenyl bridge while the LUMO is distributed over both the phenyl bridge and the triazine acceptor. For **CzpPhTrz**, the HOMO is extended significantly onto the **PCP** core owing to the strong π–π through-space interactions within the **Czp** donor. **CzPhTrz** has been previously studied where it has been reported[20] to possess a rod-like structure coupled with a ΔE_{ST} of 0.36 eV and a calculated dihedral angle between the Cz and the phenyl bridge of 51.8°. The large ΔE_{ST} for this molecule leads to inefficient TADF. Lee *et al.*[20] further showed **CzPhTrz** to be isotropic in the **DPEPO** film and so without the horizontal orientation desired to improve light outcoupling. OLEDs fabricated with this emitter (λ_{EL} = 449 nm) showed an EQE_{max} of only 4.2% (EQE_{1000} = 0.6%) despite a photoluminescence quantum yield, Φ_{PL}, of 71%. We similarly calculated a small twist angle of 51° between the donor and phenyl bridge, in a good agreement with the crystal structure analysis (45.11°, Fig. 2), and a large ΔE_{ST} of 0.38 eV in **CzPhTrz** (Fig. 3). Introduction of the rigid and sterically bulky **PCP** onto the donor in **CzpPhTrz** not only induced a larger torsion between the donor and the bridge but also extended the conjugation length. Thus, **Czp** is a stronger donor, the impact of which is a lower S_1 energy, a smaller ΔE_{ST} and a more efficient TADF process in **CzpPhTrz**. Indeed, DFT calculations predict an increased torsion of 58° (55.86° in the crystal structure), a smaller ΔE_{ST} of 0.30 eV and a lower S_1 energy of 3.11 eV compared to **CzPhTrz** [$E(S_1)$ = 3.27 eV]. The S_1 energy is nevertheless predicted to be sufficiently high such that **CzpPhTrz** should remain a good blue TADF emitter candidate.

Electrochemical properties

The HOMO and LUMO levels of **CzPhTrz** and **CzpPhTrz** were ascertained by cyclic voltammetry (CV) and differential pulse voltammetry (DPV) measurements, respectively, in dichloromethane. The CVs and DPVs are shown in Fig. S7† and data are summarized in Table 1. Both emitters possess similar reduction potentials at −1.78 V, which were assigned to the reduction of the cyaphenine acceptor. However, and in line with the theoretical studies, the oxidation potential of **CzpPhTrz** (1.14 V) is significantly cathodically shifted to that of **CzPhTrz** (1.43 V). Thus, the introduction of the **PCP** moiety appreciably reduces the ionization potential (IP) of the donor and thus the electrochemical gap. Expectedly, the oxidation waves of both compounds were found to be irreversible as the carbazole radical cation is known to be electrochemically unstable and subsequently can undergo dimerization.[21]

Photophysical properties

Fig. 4A shows the UV-Vis absorption and photoluminescence (PL) spectra of **CzPhTrz** and **CzpPhTrz** in toluene and the data

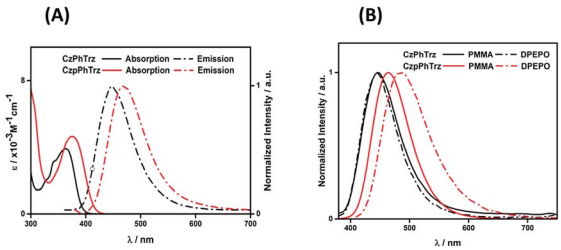

Fig. 4 (A) UV-vis absorption and PL spectra in PhMe (B) PL spectra of thin films of **CzPhTrz** and **CzpPhTrz** (λ_{exc} = 360 nm).

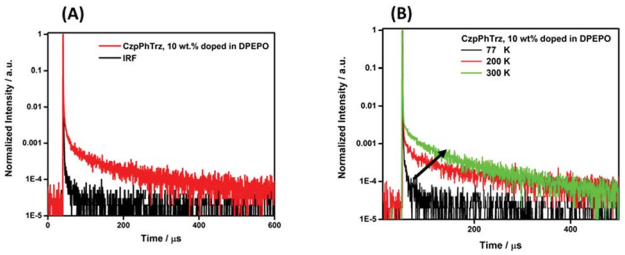

Fig. 5 (A) Time-resolved PL decay curve and (B) temperature dependence of time-resolved PL lifetime of **CzpPhTrz** in 10 wt% **DPEPO** film (λ_{exc} = 378 nm), IRF = instrument response function.

are summarized in Table 1. Both compounds possess an intramolecular charge transfer (ICT) absorption band from the carbazole-based donor to the triazine acceptor at 363 and 375 nm, respectively, for **CzPhTrz** and **CzpPhTrz**. The more intense and red-shifted band in **CzpPhTrz** agrees with the calculations shown in Fig. 3.

Both compounds exhibited unstructured PL spectra in PhMe, indicative of an excited state with strong intramolecular charge transfer (ICT) character. Analogous to their relative behavior in the ground state, the photoluminescence maximum, λ_{PL}, of **CzpPhTrz** at 470 nm is red-shifted compared to that of **CzPhTrz** ($\lambda_{PL} = 446$ nm). The Φ_{PL} values in PhMe for **CzPhTrz** and **CzpPhTrz** are 60% and 70%, which decreased to 58% and 55%, respectively, upon exposure to air. The enhanced Φ_{PL} of **CzpPhTrz** is consistent with the higher predicted oscillator strength. The time-resolved PL spectra in PhMe for both emitters (Fig. S9†), however, do not show any delayed emission,

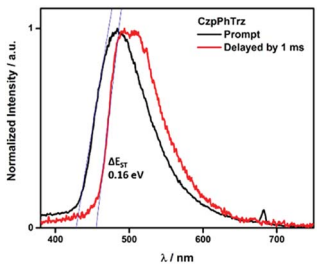

Fig. 6 Prompt and delayed spectra (at 77 K) of **CzpPhTrz** in 10 wt% **DPEPO** film ($\lambda_{exc} = 355$ nm).

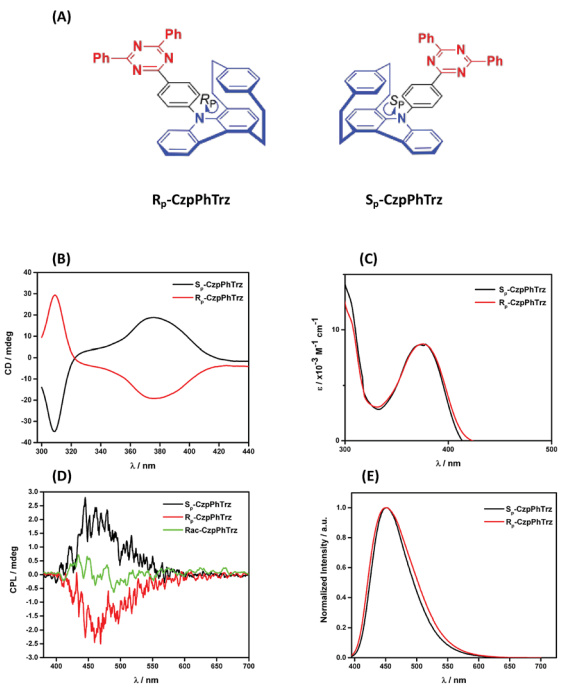

Fig. 7 (A) Chemical structures (B) CD (C) UV-vis (D) CPL and (E) PL spectra of (R_P)-**CzpPhTrz** and (S_P)-**CzpPhTrz** in degassed PhMe ($\lambda_{exc} =$ 375 nm).

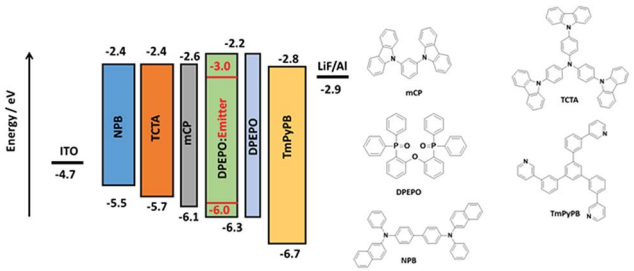

Fig. 8 Chemical structures and energy levels of materials used for the device fabrication.

which would suggest that the TADF mechanism in solution is very weak despite the oxygen sensitivity noted for Φ_{PL}.

We next investigated the PL behavior in the solid-state as doped thin films (Fig. 4B). In both PMMA and **DPEPO** matrices, both compounds showed unstructured ICT-based emission. In 10 wt% doped solution-processed PMMA films, **CzPhTrz** shows deep blue emission with λ_{PL} of 446 nm; the emission energy is essentially the same in vacuum-deposited 10 wt% doped **DPEPO** films at 448 nm. The emission of **CzpPhTrz** is expectedly red-shifted at 464 nm in PMMA, and this emission is further red-shifted to 482 nm in the more polar **DPEPO**. The Φ_{PL} values of the PMMA films of **CzPhTrz** and **CzpPhTrz** are 25% and 45%, respectively. Further, both compounds exhibited a mono exponential decay with PL lifetimes, τ of 5 ns for **CzPhTrz** and 8 ns for **CzpPhTrz**, suggesting that TADF mechanism is absent in a non-polar host like PMMA, results in line with those observed in PhMe. The much enhanced Φ_{PL} of **CzpPhTrz** is 69% in **DPEPO**, which is significantly higher than that of **CzPhTrz** ($\Phi_{PL} = 50\%$). Reducing the doping concentration to 1 wt% resulted in a lower Φ_{PL} of 43% for **CzpPhTrz** (Table S2†). Time-resolved PL measurements of the 10 wt% **DPEPO** films revealed divergent behavior between the two

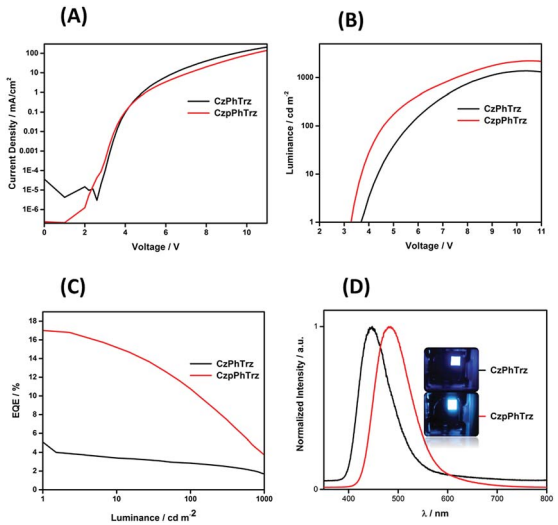

Fig. 9 (A) Current density–voltage characteristics (B) luminance *vs.* voltage. (C) EQE *vs.* luminance (D) normalized EL spectra of **CzPhTrz** and **CzpPhTrz**.

Table 2 Electroluminescence properties of CzPhTrz and CzpPhTrz

	V_{on}[a], [V]	λ_{EL}[b], [nm]	EQE_{max}[c], EQE_{100}[d], [%]	CE_{max}[c], [cd A^{-1}]	PE_{max}[c], [lm W^{-1}]	CIE[e], (x, y)
CzPhTrz	3.6	446	5.8; 2.8	10.5	8.6	(0.14, 0.12)
CzpPhTrz	3.2	480	17.0; 12.0	34.8	32.5	(0.17, 0.25)

[a] Measured at 1 cd m^{-2}. [b] Emission maxima at 1 mA cm^{-2}. [c] Maximum efficiencies at 1 cd m^{-2}. [d] EQE at 100 cd m^{-2}. [e] Commission Internationale de l'Eclairage coordinates at 1 mA cm^{-2}.

emitters. Only a nanosecond (τ = 4.8 ns) monoexponential fluorescence decay was observed for **CzPhTrz** (Fig. S10†), results that agree with the literature.[20] For **CzpPhTrz**, both prompt (τ_p = 7 ns) and delayed (τ_d = 65 μs) emission was observed (Fig. 5A). We next studied the temperature dependence of the delayed lifetime of **CzpPhTrz** (Fig. 5B). An increase in the intensity of the delayed emission as a function of increasing temperature provides corroborating evidence to support the TADF character of **CzpPhTrz**.

The ΔE_{ST} of **CzPhTrz** and **CzpPhTrz** were determined from the singlet and triplet energies estimated from the onset of the prompt and delayed emission spectra, respectively, measured in 10 wt% **DPEPO** doped films at 77 K (Fig. 6). **CzpPhTrz** possesses a high S_1 energy of 2.90 eV [$E(S_1)$ = 2.87 eV at room temperature] coupled with a small ΔE_{ST} value of 0.16 eV, confirming its strong potential as a blue TADF emitter. The turn-on of the TADF in **DPEPO** is due to preferential stabilization of the ^{1}CT state and the associated decrease in ΔE_{ST}. On the other hand, a rather large ΔE_{ST} of 0.32 eV (Fig. S11†) was determined for **CzPhTrz**, implying a much weaker TADF character. These results clearly demonstrate that the introduction of the bulky **PCP** moiety with the carbazole donor to form the carbazolophane (**Czp**) not only turns on the TADF channel in the emission mechanism in polar media, but the high Φ_{PL} is maintained.

Chiroptical properties

The ground and excited state chiroptical properties of (*R*, *S*)-**CzpPhTrz** (Fig. 7a) were studied by CD and CPL spectroscopy, respectively in toluene. As shown in Fig. 7B, there is the expected mirror image spectra corresponding to each of the two enantiomers. Using the molar extinction coefficients $\varepsilon(R)$ and $\varepsilon(S)$ (Fig. 7C) of the CT band at 375 nm, the CD dissymmetry factor was estimated to be $+5.0 \times 10^{-3}$ and -7.0×10^{-3} for the R_P and S_P enantiomers, respectively. Similarly, mirror image CPL spectra (Fig. 7D) were obtained with g_{lum} values for both R_P and S_P enantiomers at their emission maxima at 1.2×10^{-3} and 1.3×10^{-3}. These are typical values for CPL-SOMs.

Device fabrication

Based on the promising photophysical properties of ***rac*-CzpPhTrz** in **DPEPO** films, we fabricated vacuum-deposited multilayer OLEDs. A deep HOMO level of −6.06 eV for ***rac*-CzpPhTrz** was measured by UV ambient pressure photoemission spectroscopy (APS), which is deeper than that inferred from cyclic voltammetry measurements (E_{HOMO} = 5.80 eV, Table 1) by 0.26 eV, due in part to the different measurement environments (neat film for APS and DCM for DPV). Therefore, to confine the excitons in the emissive layer, **DPEPO**, with a HOMO energy of −6.3 eV was chosen as a host material in the emissive layer.[22] Optimum host and doping concentration were assessed by absolute Φ_{PL} measurements (Table S2†). An energy level diagram of the OLED stack and chemical structures of the materials used are shown in Fig. 8. The OLED architecture employed consisted of: ITO/**NPB** (30 nm)/**TCTA** (20 nm)/***m*CP** (10 nm)/***rac*-CzpPhTrz** : **DPEPO** (10 wt%, 20 nm)/**DPEPO** (10 nm)/**TmPyPB** (40 nm)/LiF (1 nm)/Al (100 nm), where *N*,*N*′-bis(naphthalen-1-yl)-*N*,*N*′-bis(phenyl)benzidine (**NPB**) was used as a hole injection layer (HIL), tris(4-carbazoyl-9-ylphenyl)amine (**TCTA**) was used as a hole transporting layer (HTL), ***m*CP** (1,3-bis(*N*-carbazolyl)benzene) and **DPEPO** were used as an electron and hole blockers, respectively. The electron transporting layer (ETL) was comprised of 1,3,5-tris(3-pyridyl-3-phenyl)benzene (**TmPyPB**), which possesses a high electron mobility of 10^{-4} cm^2 V^{-1} s^{-1} and a high triplet energy of 2.75 eV along with a deep HOMO energy of 6.7 eV.[23] We also fabricated the reference OLED using **CzPhTrz** as the emitter using the same device architecture.

The electroluminescence (EL) properties are shown in Fig. 9 and the data are summarized in Table 2. OLEDs based on **CzPhTrz** exhibited a deep blue emission with a λ_{EL} of 446 nm and CIE coordinates of (0.16, 0.12) whereas devices employing ***rac*-CzpPhTrz** showed a slightly red-shifted emission with a λ_{EL} of 480 nm and CIE coordinates of (0.17, 0.25). The EL spectra matched very well to the corresponding PL spectra. Both devices exhibited steep current-voltage-luminance behavior (Fig. 9A and B) and low turn-on voltages (V_{on}) of 3.6 V and 3.2 V for the OLEDs based on **CzPhTrz** and ***rac*-CzpPhTrz**, respectively. The lower V_{on} for the OLED with ***rac*-CzpPhTrz** is attributed to the lower energy gap of this emitter.

Fig. 9C shows the EQE *versus* luminance of the two OLEDs. The device with ***rac*-CzpPhTrz** exhibited a high EQE_{max} of 17% at low brightness (at 1 cd m^{-2}), indicating an efficient triplet harvesting in the OLED mediated by the TADF channel. Further the device showed a moderate efficiency roll-off to 12% at a display relevant brightness of 100 cd m^{-2}. Assuming the recombination efficiency to be unity and taking the Φ_{PL} of 70%, the device with ***rac*-CzpPhTrz** possessed an outcoupling efficiency of 25%. On the other hand, devices based on **CzPhTrz** showed an EQE_{max} of 5.8% at low brightness, which reduced to 2.8% at 100 cd m^{-2}. The significantly poorer performance is due in part to the larger ΔE_{ST} of the emitter, which renders TADF very inefficient in the device. To summarize, we observed a three-fold enhancement in the

EQE_{max} as a function of the use of the **Czp** donor in ***rac*-CzpPhTrz**. To the best of our knowledge, the OLED with ***rac*-CzpPhTrz** is the first example of an EL device incorporating a [2.2] paracyclophane moiety. ***rac*-CzpPhTrz** indeed is amongst the state-of-the art blue to sky-blue TADF triazine-based emitters in terms of EQE_{max} though at a cost of a red-shifted EL spectrum compared to OLEDs based on emitters shown in Fig. 1.

Conclusion

In conclusion, we have demonstrated how TADF and CPL can be turned on in triazine emitters through incorporation of a [2.2] paracyclophane moiety within the carbazole donor structure. The resulting carbazolophane (**Czp**) donor unit both provides a through-space π–π interaction and an increased torsion as a function of the increased inherent bulkiness of the donor. This enhances the donor strength and forces a larger torsion between the donor and the phenyl bridge, leading to a much more efficient TADF process. Moreover, the enantiomers possessed mirror image CD and CPL spectra with g_{lum} in line with other CPL-SOMs. The resulting sky-blue OLED showed a three-fold enhancement in performance compared to the reference device with EQE_{max} of 17%. These results demonstrate clearly the value of the **Czp** donor, which we believe can be applied to a whole range of TADF emitters to enhance OLED and CPL performance.

Conflicts of interest

There are no conflicts to declare.

Acknowledgements

We are grateful to the EPSRC for financial support (grants EP/P010482/1, EP/R035164/1 and EP/L017008/1). We thank the EPSRC UK National Mass Spectrometry Facility at Swansea University for analytical services. E. Z.-C. thanks the University of St Andrews for support. E. S. and S. B. acknowledge funding from DFG in the frame of SFB1176 (projects A4, B3 and C6) and KSOP (fellowship to E. S.). C. M. M. greatly acknowledges financial support by the cluster of excellence (3DMM2O). We are grateful to JST-ERATO for financial support (grant JPMJER1305). We thank the JSPS Core-to-Core Program for financial support. The measurement of CPL was made using CPL-200 (JASCO) at the Natural Science Center for Basic Research and Development (N-BARD), Hiroshima University.

Notes and references

§ Synthesis, NMR spectra, elemental analysis data, TGA and DSC, cyclic voltammetry data, supplementary photophysical measurements, computational data, electroluminescence data and crystallographic data (CCDC-1871934 and CCDC-1871935). During the proofs stage it has been pointed out to us that the structure and synthesis of CzpPhTRZ has appeared in a patent: Buchwald, S. L.; Huang, W., "[2.2]Paracyclophane-Derived Donor/Acceptor-Type Molecules for OLED Applications", Massachusetts Institute of Technology, International Patent application number PCT/US2016/035655, published 8 December 2016.

1 (*a*) Z. Yang, Z. Mao, Z. Xie, Y. Zhang, S. Liu, J. Zhao, J. Xu, Z. Chi and M. P. Aldred, *Chem. Soc. Rev.*, 2017, **46**, 915–1016; (*b*) M. Y. Wong and E. Zysman-Colman, *Adv. Mater.*, 2017, **29**, 1605444; (*c*) Y. Liu, C. Li, Z. Ren, S. Yan and M. R. Bryce, *Nat. Rev. Mater.*, 2018, **3**, 18020.
2 (*a*) L. S. Cui, H. Nomura, Y. Geng, J. U. Kim, H. Nakanotani and C. Adachi, *Angew. Chem., Int. Ed. Engl.*, 2017, **56**, 1571–1575; (*b*) Y.-C. Duan, L.-L. Wen, Y. Gao, Y. Wu, L. Zhao, Y. Geng, G.-G. Shan, M. Zhang and Z.-M. Su, *J. Phys. Chem. C*, 2018, **122**, 23091–23101.
3 W. Huang, M. Einzinger, T. Zhu, H. S. Chae, S. Jeon, S.-G. Ihn, M. Sim, S. Kim, M. Su, G. Teverovskiy, T. Wu, T. Van Voorhis, T. M. Swager, M. A. Baldo and S. L. Buchwald, *Chem. Mater.*, 2018, **30**, 1462–1466.
4 Y. Wada, S. Kubo and H. Kaji, *Adv. Mater.*, 2018, **30**, 1705641.
5 Q. Zhang, B. Li, S. Huang, H. Nomura, H. Tanaka and C. Adachi, *Nat. Photonics*, 2014, **8**, 326–332.
6 W.-L. Tsai, M.-H. Huang, W.-K. Lee, Y.-J. Hsu, K.-C. Pan, Y.-H. Huang, H.-C. Ting, M. Sarma, Y.-Y. Ho, H.-C. Hu, C.-C. Chen, M.-T. Lee, K.-T. Wong and C.-C. Wu, *Chem. Commun.*, 2015, **51**, 13662–13665.
7 W. Li, X. Cai, B. Li, L. Gan, Y. He, K. Liu, D. Chen, Y.-C. Wu and S.-J. Su, *Angew. Chem., Int. Ed.*, 2019, **58**, 582–586.
8 C. Wang, H. Fei, Y. Qiu, Y. Yang, Z. Wei, Y. Tian, Y. Chen and Y. Zhao, *Appl. Phys. Lett.*, 1999, **74**, 19–21.
9 T. Harada, H. Hayakawa, M. Watanabe and M. Takamoto, *Rev. Sci. Instrum.*, 2016, **87**, 075102.
10 B. C. Kim, Y. J. Lim, J. H. Song, J. H. Lee, K. U. Jeong, J. H. Lee, G. D. Lee and S. H. Lee, *Opt. Express*, 2014, **22**(Suppl. 7), A1725–A1730.
11 E. M. Sanchez-Carnerero, A. R. Agarrabeitia, F. Moreno, B. L. Maroto, G. Muller, M. J. Ortiz and S. de la Moya, *Chemistry*, 2015, **21**, 13488–13500.
12 T. Imagawa, S. Hirata, K. Totani, T. Watanabe and M. Vacha, *Chem. Commun.*, 2015, **51**, 13268–13271.
13 S. Feuillastre, M. Pauton, L. Gao, A. Desmarchelier, A. J. Riives, D. Prim, D. Tondelier, B. Geffroy, G. Muller, G. Clavier and G. Pieters, *J. Am. Chem. Soc.*, 2016, **138**, 3990–3993.
14 M. Li, S. H. Li, D. Zhang, M. Cai, L. Duan, M. K. Fung and C. F. Chen, *Angew. Chem., Int. Ed. Engl.*, 2018, **57**, 2889–2893.
15 F. Song, Z. Xu, Q. Zhang, Z. Zhao, H. Zhang, W. Zhao, Z. Qiu, C. Qi, H. Zhang, H. H. Y. Sung, I. D. Williams, J. W. Y. Lam, Z. Zhao, A. Qin, D. Ma and B. Z. Tang, *Adv. Funct. Mater.*, 2018, **28**, 1800051.
16 M. Y. Zhang, Z. Y. Li, B. Lu, Y. Wang, Y. D. Ma and C. H. Zhao, *Org. Lett.*, 2018, **20**, 6868–6871.
17 E. Spuling, N. Sharma, I. D. W. Samuel, E. Zysman-Colman and S. Bräse, *Chem. Commun.*, 2018, **54**, 9278–9281.
18 P. Lennartz, G. Raabe and C. Bolm, *Isr. J. Chem.*, 2012, **52**, 171–179.
19 H. Wolf, D. Leusser, M. R. V. Jørgensen, R. Herbst-Irmer, Y.-S. Chen, E.-W. Scheidt, W. Scherer, B. B. Iversen and D. Stalke, *Chem.–Eur. J.*, 2014, **20**, 7048–7053.
20 S. Y. Byeon, J. Kim, D. R. Lee, S. H. Han, S. R. Forrest and J. Y. Lee, *Adv. Opt. Mater.*, 2018, **6**, 1701340.

21 (*a*) A. Tomkeviciene, J. V. Grazulevicius, D. Volyniuk, V. Jankauskas and G. Sini, *Phys. Chem. Chem. Phys.*, 2014, **16**, 13932–13942; (*b*) T. Fukushima, J. Yamamoto, M. Fukuchi, S. Hirata, H. H. Jung, O. Hirata, Y. Shibano, C. Adachi and H. Kaji, *AIP Adv.*, 2015, **5**, 087124.

22 C. Han, Y. Zhao, H. Xu, J. Chen, Z. Deng, D. Ma, Q. Li and P. Yan, *Chem.–Eur. J.*, 2011, **17**, 5800–5803.

23 S.-J. Su, T. Chiba, T. Takeda and J. Kido, *Adv. Mater.*, 2008, **20**, 2125–2130.